JMEPEG (2017) 26:4265–4273
DOI: 10.1007/s11665-017-2912-3

1059-9495/$19.00

Superplastic Forming/Diffusion Bonding Without Interlayer of 5A90 Al-Li Alloy Hollow Double-Layer Structure

Shaosong Jiang, Yong Jia, Zhen Lu, Chengcheng Shi, and Kaifeng Zhang

(Submitted December 30, 2016; in revised form July 3, 2017; published online September 5, 2017)

The hollow double-layer structure of 5A90 Al-Li alloy was fabricated by SPF/DB process in this study. The characteristics and mechanism of 5A90 Al-Li alloy with respect to superplasticity and diffusion bonding were investigated. Tensile tests showed that the optimal elongation of tensile specimens was 243.97% at the temperature of 400 °C and the strain rate of 0.001 s^{-1}. Effect of the surface roughness, bonding temperature and bonding time to determine the microstructure and mechanical properties of diffusion bonding joints was investigated, and the optimum bonding parameters were 540 °C/2.5 h/Ra18. Through the finite element simulation, it could be found that the SPF/DB process of hollow double-layer structure was feasible. The hollow double-layer structure of 5A90 Al-Li alloy was manufactured, showing that the thickness distribution of the bonding area was uniform and the thinnest part was the round corner. The SEM images of diffusion bonding joints showed that sound bonding interfaces were obtained in which no discontinuity existed.

Keywords 5A90 Al-Li alloy, diffusion bonding, superplastic forming, surface roughness

1. Introduction

In recent years, the demand for lightweight structural components in the aerospace, rail transportation, automotive products and other industrial areas is increasing, and aluminum alloy has been widely used among nonferrous metals (Ref 1-4). Aluminum–lithium alloy is becoming a promising member of aluminum alloys due to its low density, high specific strength, high specific stiffness, excellent low-temperature performance, good corrosion resistance and excellent superplastic forming performance (Ref 5, 6). Therefore, it is necessary to study the superplastic forming/diffusion bonding (SPF/DB) process of aluminum–lithium components.

Superplastic forming/diffusion bonding (SPF/DB) is a technique allowing for manufacturing complex-shaped hollow metallic parts and has great advantages in reducing the weight of the structure and production costs (Ref 7, 8). Diffusion bonding of Al-Li alloy is always a tough task due to the tenacious surface oxide, which impedes metal-to-metal contact. The difficulty mainly arises from the fact that a tenacious, thin surface oxide forms readily on aluminum that acts as an effective barrier for interdiffusion and prevents metallurgical bonding between samples. To produce a sound joint, high temperature, large deformation and protective gas are generally needed (Ref 9). The technique generally used for diffusion bonding of Al-Li alloys is to combine mechanical and chemical methods to clean sample surfaces, followed by plating a thin layer (~10 μm) of transient liquid-phase (TLP) forming elements, and then performing diffusion bonding in an ambient atmosphere.

Many scholars have researched the superplasticity and/or diffusion bonding of Al-Li alloy. Zhang et al. (Ref 10) analyzed the microstructural evolution of 5A90 Al-Li alloy during superplastic deformation at the temperature of 475 °C and the initial strain rate of 8×10^{-4} s^{-1} to clarify the deformation mechanism. Huang et al. (Ref 11) investigated the application of the organic solution to form a protective layer on an oxide-free surface and analyzed the bonding mechanism for 7075 aluminum alloy. Wu studied the influence of temperature, time, deformation and microstructure for the joint effect on a superplastic 8090 aluminum alloy (Ref 12). Gilmore et al. (Ref 13) researched the origin of microstructures and the measured shear strengths of joints produced by solid-state and transient liquid-phase diffusion bonding techniques between 8090 AI-Li alloy sheets. Because of the complex nature of the SPF/DB or DB process, these studies mentioned above were limited in long-scale application.

In this paper, the superplastic properties as well as diffusion bonding characteristics of 5A90 Al-Li alloy were studied. The superplastic properties of 5A90 Al-Li alloy were obtained by tensile test under different deformation temperatures and strain rates. The effect of temperature, holding time and surface roughness to improve the bonding ratio without interlayer was investigated in this paper. Shear tests were conducted to evaluate the mechanical properties of joints. Based on tensile test results at high temperature, the superplastic forming process of hollow double-layer structure was simulated. Finally, the thickness distribution and diffusion bonding interfaces of the hollow double-layer structure were analyzed.

Shaosong Jiang, Yong Jia, Zhen Lu, Chengcheng Shi, and **Kaifeng Zhang**, National Key Laboratory of Precision Hot Processing of Metals, School of Materials Science and Engineering, Harbin Institute of Technology, Harbin 150001, China. Contact e-mail: hitjiayong@163.com.

2. Experimental

The starting material utilized in this study was hot-rolled 5A90 Al-Li alloy sheet with a thickness of 1.3 mm, and the microstructure consisted of aluminum solid solution, α phase and intermetallic compound, δ phase, as seen in Fig. 1. The chemical compositions (wt.%) of 5A90 Al-Li alloy are shown in Table 1.

Tensile specimens with a gauge length of 15 mm and gauge width of 6 mm were sectioned in the rolling direction using wire electrical discharge machining; tensile tests were performed on the Instron-5500R testing machine at the temperature ranging from 340 to 490 °C and the strain rate ranging from 1×10^{-4} s^{-1} to 1×10^{-3} s^{-1}. Then, the diffusion bonding samples were polished by sandpapers with different grits. Grit sizes of 600, 800 and 1000, respectively, corresponded to roughness parameters Ra, where Ra is the arithmetic average of the absolute values of surface roughness from the mean line, were 23, 18, and 13 μm. The specimens finally were ultrasonically cleaned in alcohol solution for 3 min.

Diffusion bonding process was carried out in the ZRY55 vacuum hot-press furnace, the vacuum degree during the experiment was 2×10^{-2} Pa, and the schematic of diffusion bonding device is presented in Fig. 2. The surface roughness, holding temperature and holding time were taken as the diffusion bonding parameters. The surface roughness was designed as 23, 18, and 13 μm, holding temperature 520, 540, and holding time 2, 2.5, and 3 h.

Shear tests for diffusion bonding joints were conducted on the Instron-5500R testing machine, where the punch pressed against the specimen at a constant rate 1 mm/min and the narrower part of the specimen cannot move due to the fixing of the mold, while the wider part of the specimen moved downward by the upper punch. The narrower and the wider part of the specimen separated gradually, and the maximum pressure in this process was the shear strength of the bonding joints, and the schematic of the shear punch die is presented in Fig. 3.

The hollow double-layer structure for 5A90 Al-Li alloy was formed by superplastic forming/diffusion bonding tech on the 200 kN hydraulic press. For the SPF/DB process, the first step was the superplastic deformation of the cavity and the other was the diffusion bonding of the contact area.

The microstructures of specimens after tensile testing were characterized with the optical microscope (OM). The fracture surface and microstructure of specimens after diffusion bonding, bonding interface of joints and post-SPF/DB part were measured by scanning electron microscope (SEM) on Quanta 200 FEG-SEM machine.

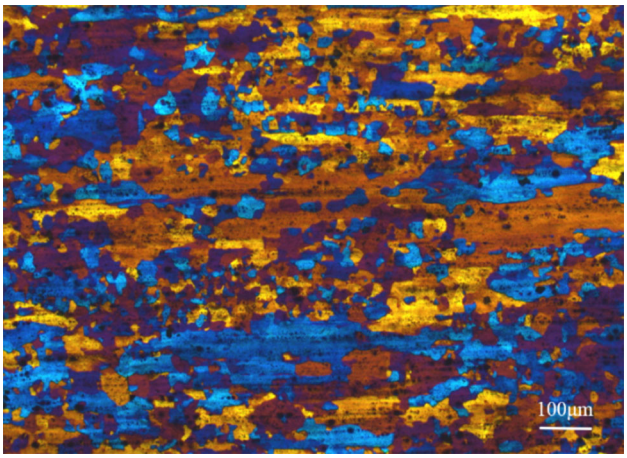

Fig. 1 Microstructure of 5A90 Al-Li alloy

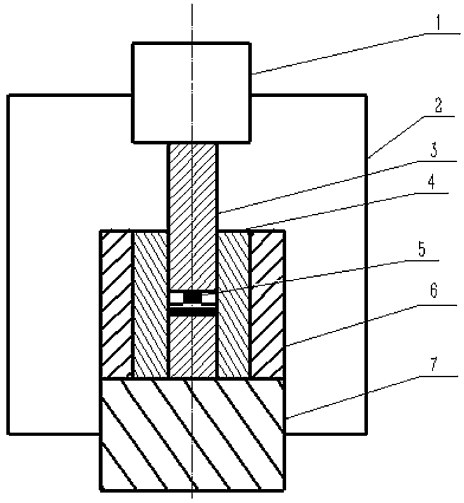

Fig. 2 Schematic illustration of diffusion bonding device

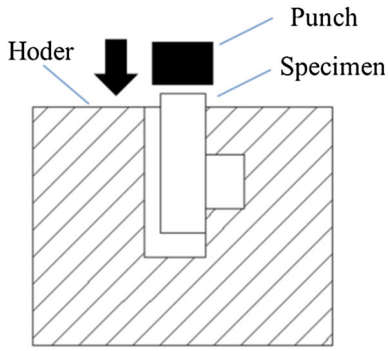

Fig. 3 Schematic illustration of the shear punch die

Table 1 Chemical composition of 5A90 Al-Li alloy

Alloy element	Li	Zr	Ti	Si	Na	Fe	Mg	Cu	Al
Wt.%	2.13	0.12	0.10	0.3-1.0	0.0005	0.075	5.34	0.051	Balance

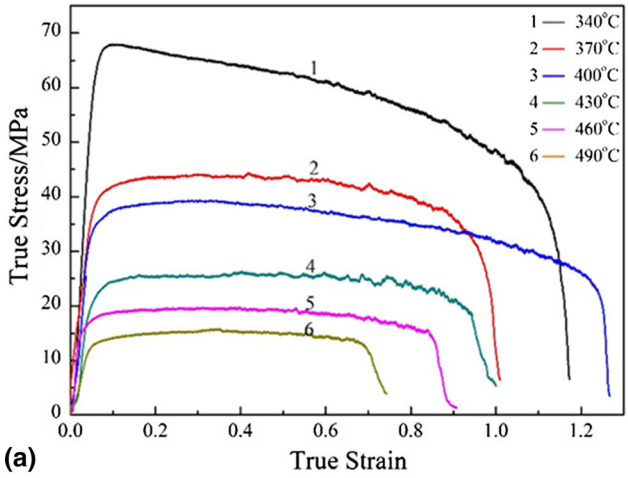

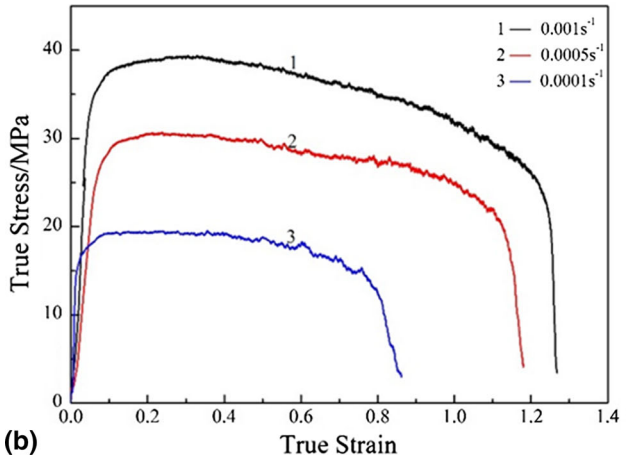

Fig. 4 The true stress–true strain curves: (a) at the strain rate of 0.001 s^{-1} with the temperature ranging from 340 to 490 °C (b) at the temperature of 400 °C with the initial strain rate ranging from 0.0001 to 0.001 s^{-1}

3. Results and Discussion

3.1 The Superplastic Property of 5A90 Al-Li Alloy at the Elevated Temperature

Figure 4 gives the true stress-true strain curves for the 5A90 Al-Li alloy at different temperatures and strain rates. As seen from Fig. 4(a), the optimal elongation of 5A90 Al-Li alloy was 243.97% at the temperature of 400 °C and the strain rate of 0.001 s^{-1}, showing excellent ductility. The flow stress decreased with the increasing temperature, and stress–strain curves exhibited flow softening behavior after the flow stress peaked. With the deformation continuing, the flow stress of the alloy entered the steady-state flow region. Because the dynamic recovery or recrystallization came to a dynamic balance with work hardening of the material (Ref 14), stress–strain curves tend to be levelled. It can be seen from Fig. 4(b) that as the strain rate decreased, there was a general trend toward lower ductility; the curve shifted higher with increasing strain rate, which can be described by a power law:

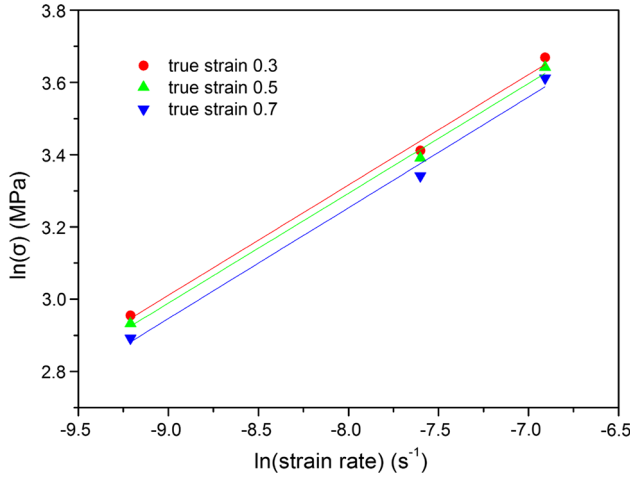

Fig. 5 Plot of ln(σ) vs. ln(strain rate) to determine the strain rate sensitivity, m, at different true strain values

Table 2 Strain rate sensitivity values for the as-received specimens

True strain	m
0.3	0.3066
0.5	0.30546
0.7	0.30395

$$\sigma = K\dot{\varepsilon}^m \quad \text{(Eq 1)}$$

where σ is the flow stress, K is a constant and m is the strain rate sensitivity exponent.

Figure 5 shows the curve of ln(σ) versus ln(strain rate) at different true strain values at 400 °C, where the slope indicates the strain rate sensitivity exponent m. The calculated strain rate sensitivity is shown in Table 2; it can be seen that the strain rate sensitivity exponent decreased with the increasing true strain. During tensile deformation, the effect of the high strain rate sensitivity, m, is to inhibit catastrophic necking. The m values of superplastic alloys generally lie in the range of 0.3 to 0.9 (Ref 15).

Figure 6 depicts the microstructure of the specimens after tensile tests at different temperatures, and the arrow in Fig. 6 indicates the tensile direction. The grains of 5A90 Al-Li alloy was obviously elongated along with the tensile direction. Figure 7 shows that the fracture morphology of the tensile sample appeared to be cavities with features of ductile fracture. The presence of cavities was detrimental to the elongation of the alloy; the nucleation and coalescence of cavities resulted in sample fracture (Ref 16). Thus, the final fracture was caused by the evolution of cavities at grain boundaries, and in this sense, cavities led to premature failure of test samples.

3.2 The Shear Strength and Microstructure of the Bonding Joints

There are many factors affecting the diffusion bonding strength of 5A90 Al-Li alloy. Effect of the bonding

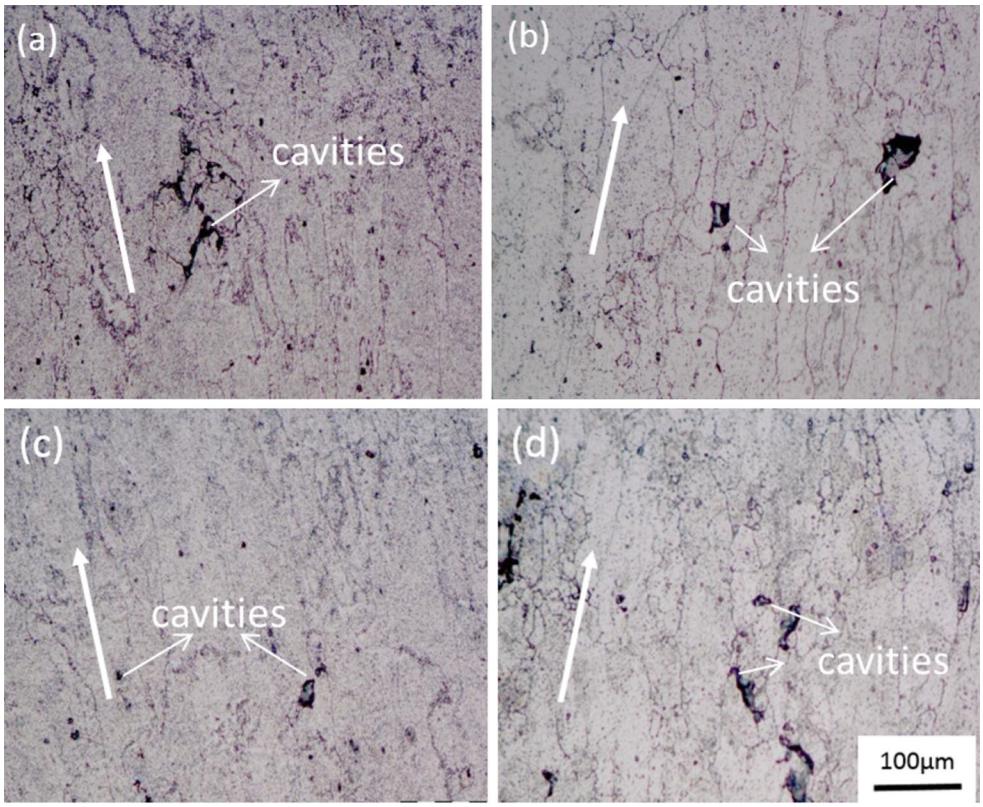

Fig. 6 Microstructure of the specimens after tensile tests at different temperatures under the initial strain rate of 0.0005 s^{-1}: (a) 400 °C, (b) 430 °C, (c), 460 °C and (d) 490 °C

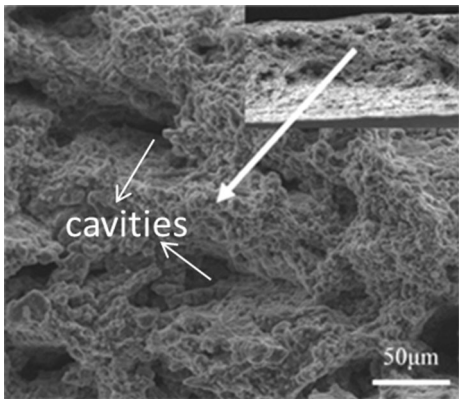

Fig. 7 The fracture morphology of the specimen at 400 °C under the strain rate of 0.001 s^{-1}

temperature, bonding time and surface roughness were investigated in this paper. Bonding temperatures ranging from 520 to 540 °C and bonding time from 2 to 3 h were used in this study. The surfaces of the samples were polished by sandpapers with grits size of 600, 800, and 1000, respectively, to design different surface roughness. The bonding pressure was set 15 MPa in the diffusion bonding process.

The microstructures of bond interface for 5A90 Al-Li alloy with different bonding parameters are observed in Fig. 8. The SEM images of Fig. 8(a) and (b) indicated that the bonding ratio of joints increased as the temperature rose. There were pronounced unconnected areas on the diffusion interface at 520 °C, and diffusion at 540 °C enhanced the bonding effect. Figure 8(b) and (c) demonstrated the effect of bonding time. It was found that a linear region consisted by some small voids existed at the bond interface for a pressing time of 2.5 h, and extending the bonding time to 3 h improved the atomic diffusion and increased the bonding area.

The surface roughness is vital for diffusion bonding. The mechanism of diffusion bonding in this paper is that the ductility of the oxide layer is different from that of Al-Li alloy. Under the same deformation conditions, the aluminum oxide layer on diffusing interface breaks firstly due to the localized crushing, and the Al-Li base material contacts at the cracked position. The cracked position further exposes with the bonding temperature and holding time increasing. Finally, the oxide layer is completely broken, gradually disappears, and a sound-bonded interface is obtained.

The bonding effect of Ra18 in Fig. 8(d) was better than that of Ra23 in Fig. 8(c) and Ra13 in Fig. 8(e), while there were voids on the interface. The microscopic evolution of surface asperities on the surface is presented in Fig. 9. The diffusion bonding interface did not provide sufficient contact region with surface roughness Ra23, so the discontinuity-bonded connection could be seen in Fig. 8(c). For the surface roughness of Ra13, discontinuity area was apparently found at the bond

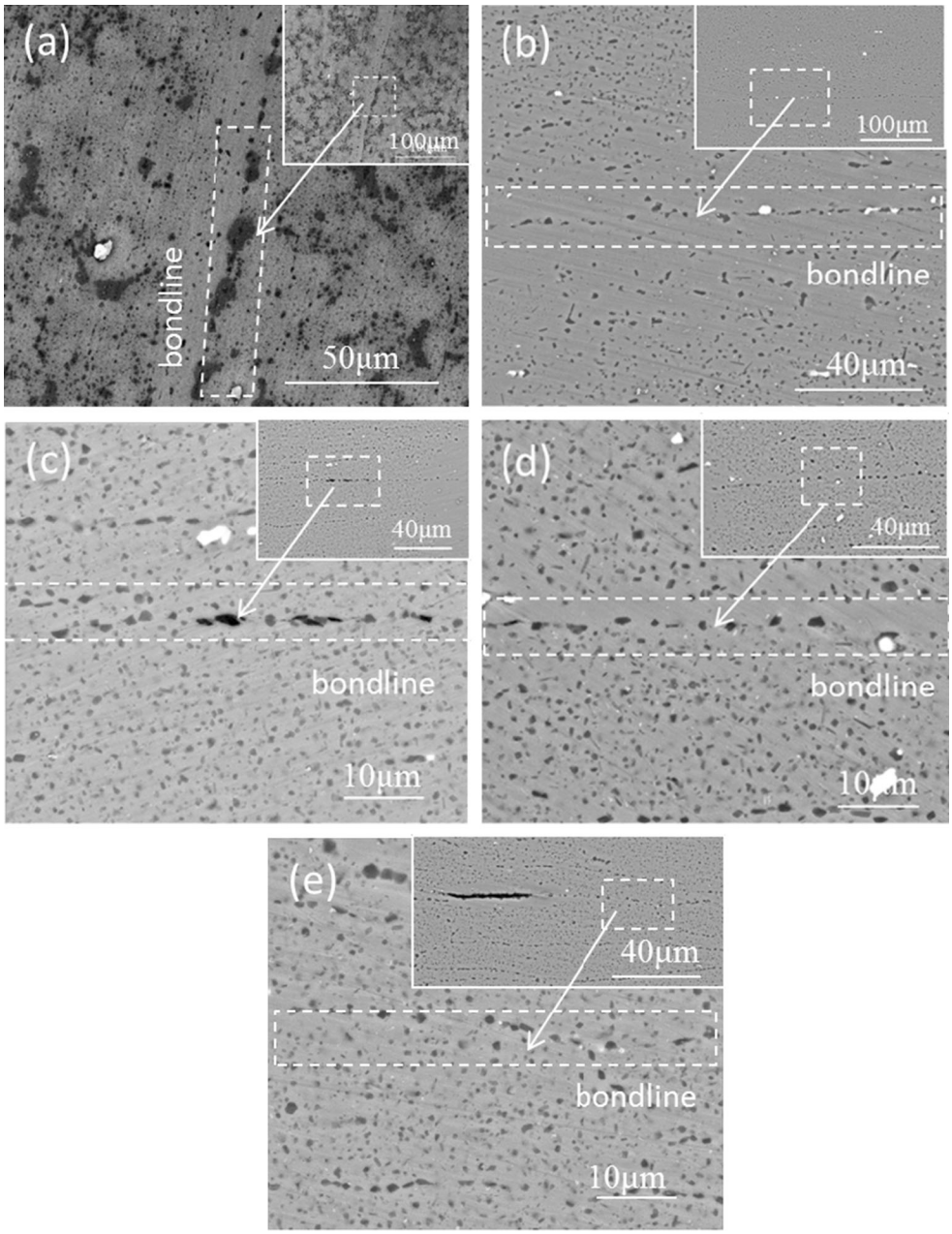

Fig. 8 Microstructure of bond interface at different bonding parameters: (a) 520 °C-2.5h-Ra23, (b) 540 °C-2.5h-Ra23, (c) 540 °C-3h-Ra23, (d) 540 °C-3h-Ra18 and (e) 540 °C-3h-Ra13

interface. As the surface roughness, Ra13 was considerably smooth, the micro-plastic deformation on the bond interface was insufficient for the ruptures of the oxide layer that impedes the atoms diffusion. Microscopic plastic deformation of the aluminum oxide layer provided the insufficient contact for the base material on the interfacial area, which resulted in discontinuity connection at this stage. Surface roughness Ra18 was appropriate for the required micro-plastic deformation considering the bonding condition.

Shear tests were conducted at room temperature to evaluate the mechanical property of joints. It could be seen from Fig. 10 that the shear strength increased with the holding time, and the extension of the time promoted the atoms diffusion at the interface, which improved the bonding ratio. The shear strength decreased gradually with the increase in the diffusion temperature in a certain range. Grain coarsening around the bond interface was perhaps the principal reason for the drop of shear strength (Ref 4, 9).

The shear strength of the Ra18 was larger than that of joints bonded at Ra23 and Ra13. The larger surface roughness could not provide sufficient contact region for the plastic deformation of the oxide layer on loading, and the oxide layer would severely hinder the diffusion of atoms, resulting in the decrease in the shear stress. When the surface roughness was smaller, the diffusion bonding interface had a smooth surface, which reduced the micro-plastic deformation area. The reduction in

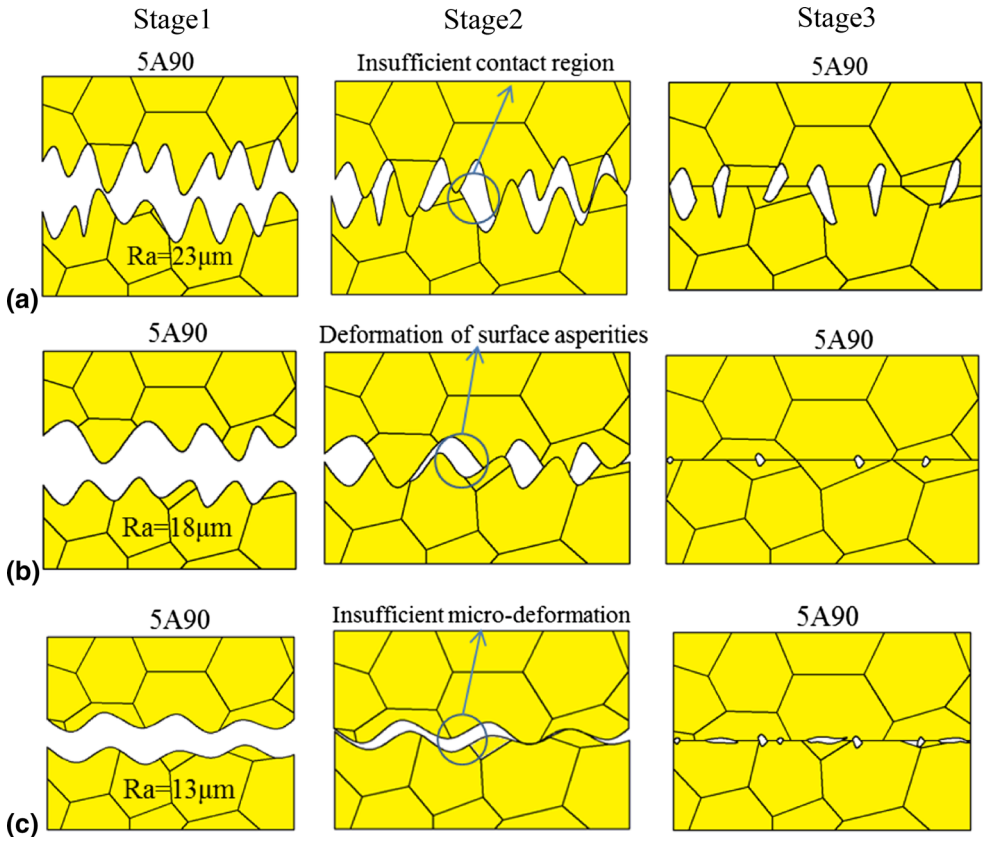

Fig. 9 Microscopic evolution of surface asperities: (a) Ra23 μm, (b) Ra18 μm and (c) Ra13 μm

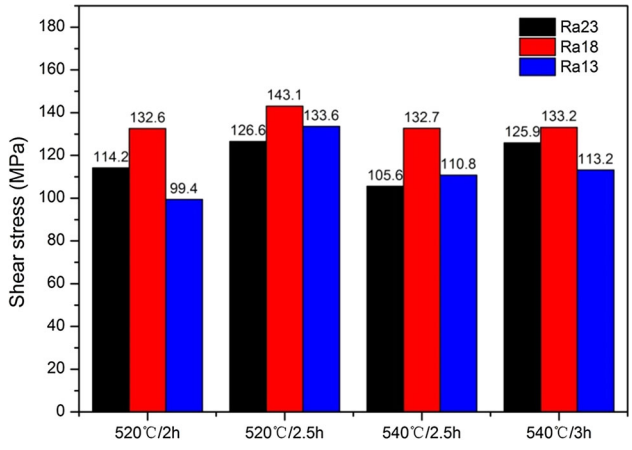

Fig. 10 The shear strength of joints bonded at different bonding parameters

micro-plastic deformation region was adverse to the rupture of the oxide layer. It was found that when the surface roughness was Ra18, the shear strength of bonding joints was larger than others, so the surface roughness Ra18 was adopted in the SPF/DB process. The highest bonding shear strength achieved was 143.1 MPa under the condition of holding at 520 °C for 150 min with surface roughness Ra18.

3.3 The Finite Element Analysis of the Hollow Double-Layer Structure

Figure 11 shows the finite element analysis (FEA) of the thickness distribution of the hollow double-layer structure with time. It was known in section 3.2 that 5A90 Al-Li alloy exhibited superplasticity under the strain rate of 0.001 s^{-1}, so the strain rate for FEA was set 0.001 s^{-1}; then, the die was set rigid. The boundary conditions imposed on the diffusion bonding area before the simulation to ensure that there will be no displacement change in the bonding joints. The area, where the boundary conditions were not imposed and finite element mesh division was dense, was the deformed part. The middle part of the cavities deformed and fitted the mold firstly in superplastic deformation. The round corner, which required larger forming force, deformed at last and was the thinnest part of the hollow double-layer structure. The thickness of the reinforcing rib varied greatly, which was formed by the superplastic bulging of cavities. The reinforcing ribs subjected to tensile stress, resulting in thinning of the structural thickness.

The thickness distribution of the sheet is shown in Fig. 12. The numerical simulation results predicted that there was no significant change in the thickness of the whole sheet, and the maximum thinning rate of the hollow double-layer structure was 35% at the round corner. Due to the limitation of the boundary conditions, the reduction in the blank changed little, and the thinning rate of the reinforcing ribs was the fastest.

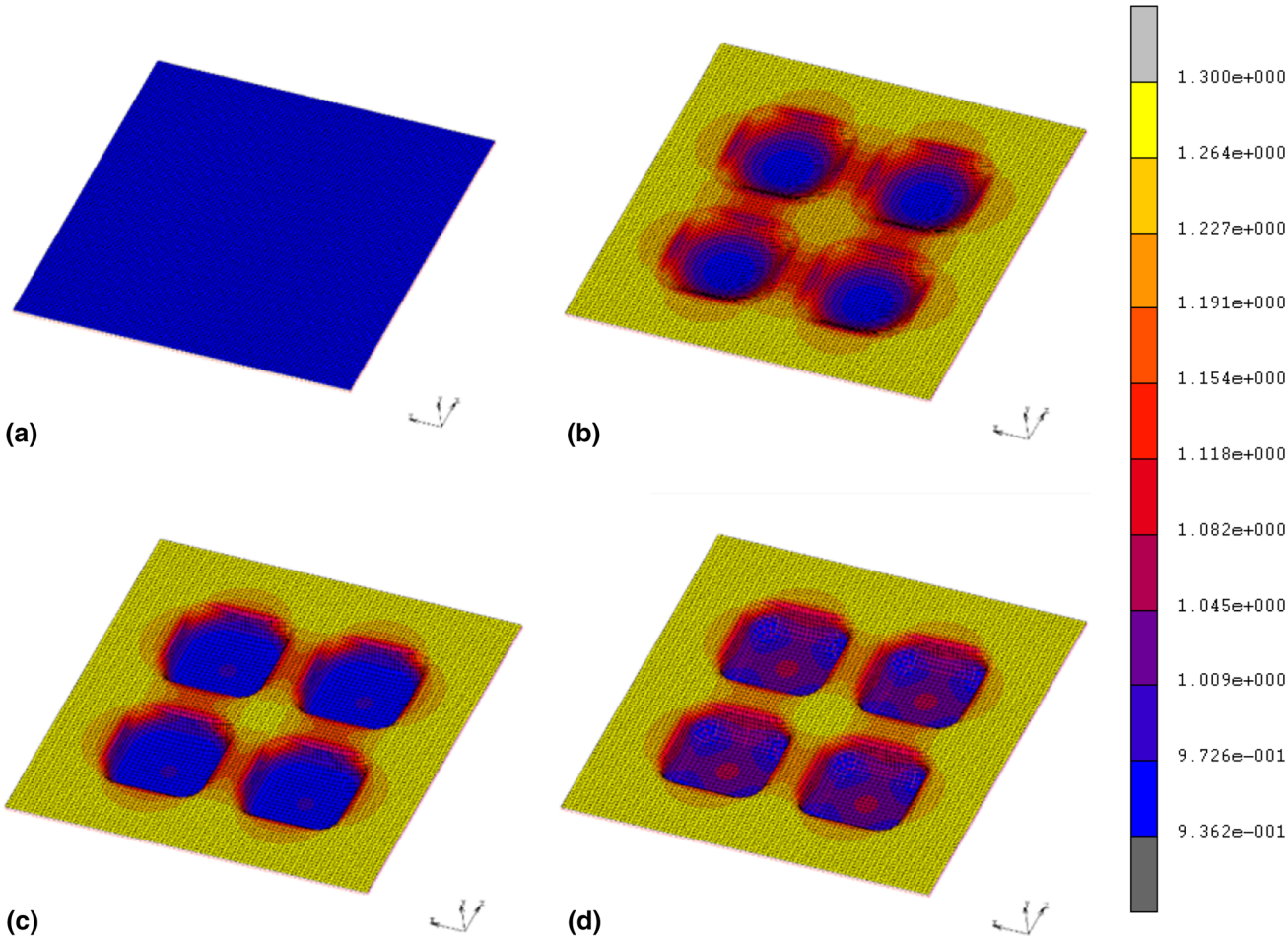

Fig. 11 The thickness distribution of the hollow double-layer structure with time: (a) t = 0 s, (b) t = 240 s, (c) t = 480 s and (d) t = 780 s

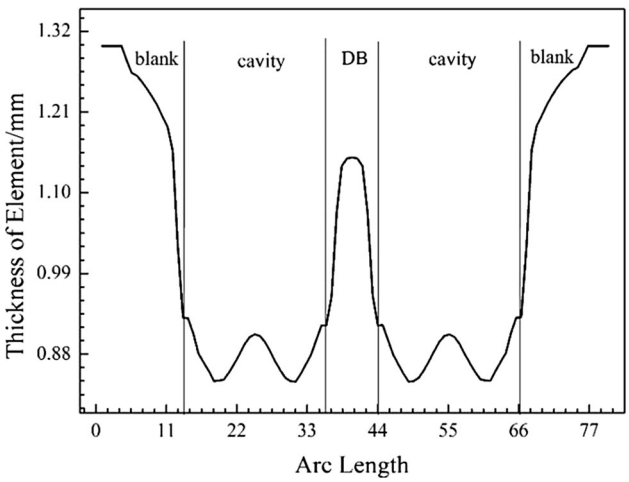

Fig. 12 The thickness distribution of the sheet by FEA

3.4 The Superplastic Forming/Diffusion Bonding of Hollow Double-Layer Structure

The optimal superplastic temperature of the 5A90 Al-Li alloy was 400 °C, and the optimum diffusion bonding temperature of the 5A90 Al-Li alloy was about 520 °C. Therefore, the superplastic forming process was carried out in the ZRY55 vacuum hot-press furnace at first, and then, the diffusion bonding process was performed. The hollow double-layer structure of 5A90 Al-Li alloy fabricated by SPF/DB process is shown in Fig. 13.

To keep the forming pressure constant, sheets were sealed before putting into the 200KN hydraulic press. Boron nitride applied on the concave die played a role in lubrication and antioxidation. The mold and the sheet were heated to the superplastic forming temperature for a certain time, and then, the argon gas was introduced. The high-pressure argon gas maintained for some time until the sheet contacted with the concave mold. The diffusion bonding process was the second

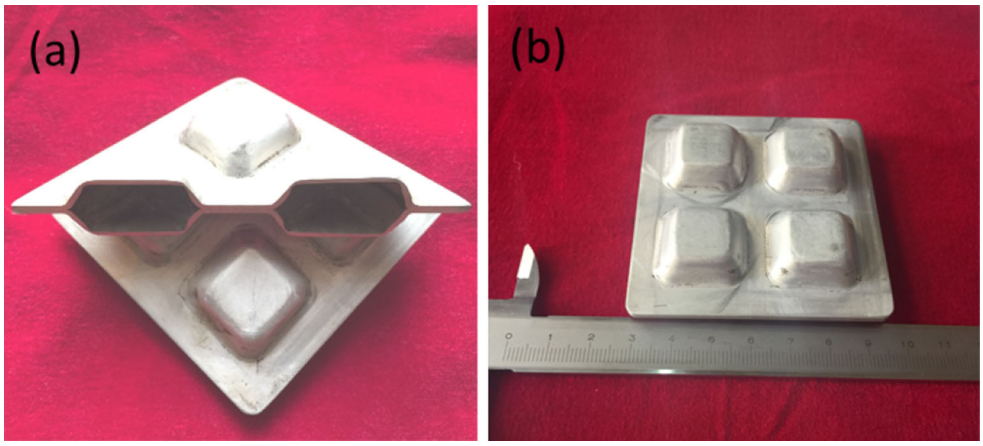

Fig. 13 The hollow double-layer structure of 5A90 Al-Li alloy fabricated by SPF/DB

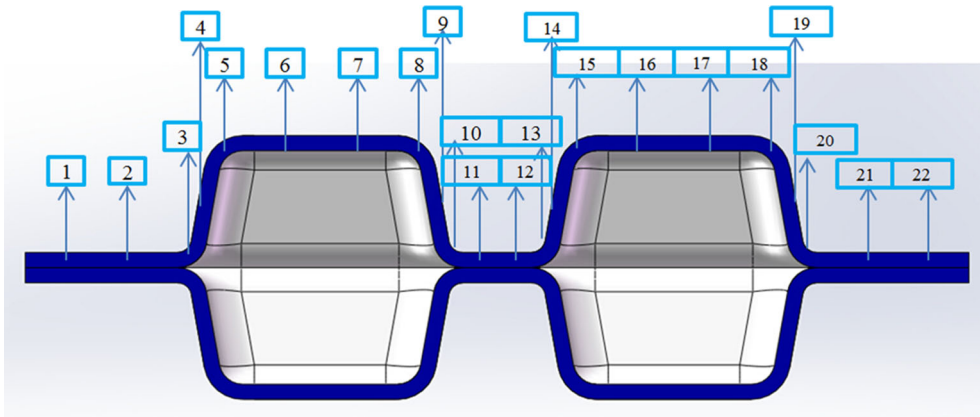

Fig. 14 The cross section of the final component with thickness measurement points

Table 3 The thickness of finished structure at different points

IDS	1	2	3	4	5	6	7	8	9	10	11
Thickness, mm	1.28	1.26	1.10	1.20	0.82	1.16	1.14	0.78	1.10	1.08	1.24
IDS	**12**	**13**	**14**	**15**	**16**	**17**	**18**	**19**	**20**	**21**	**22**
Thickness, mm	1.26	1.06	1.10	0.84	1.12	1.14	0.8	1.10	1.06	1.26	1.26

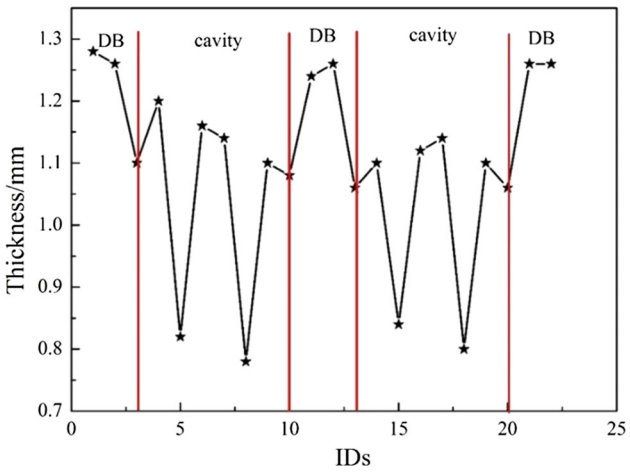

Fig. 15 The thickness distribution of the final component

step. The temperature in the furnace was raised to the diffusion bonding temperature, and the pressure was applied to the bonding area by the upper and lower indenter. The diffusion bonding process maintained at a pressure of 15 MPa and a holding time of 2.5 h to assure the bonding was sufficient.

3.4.1 The Thickness Distribution. The thickness distribution matters which affects the structural strength. The measurement points are shown in Fig. 14. All the data of thickness are listed in Table 3. Figure 15 shows the thickness distribution of the final component.

It can be seen from Fig. 15 that the overall thickness distribution of the hollow double-layer structure fluctuated greatly and the thickness of the diffusion bonding zone had changed little. The area where the thickness reduced was mainly concentrated on the cavities, and the thickness severely reduced at the round corner with the maximum thinning rate 38%.

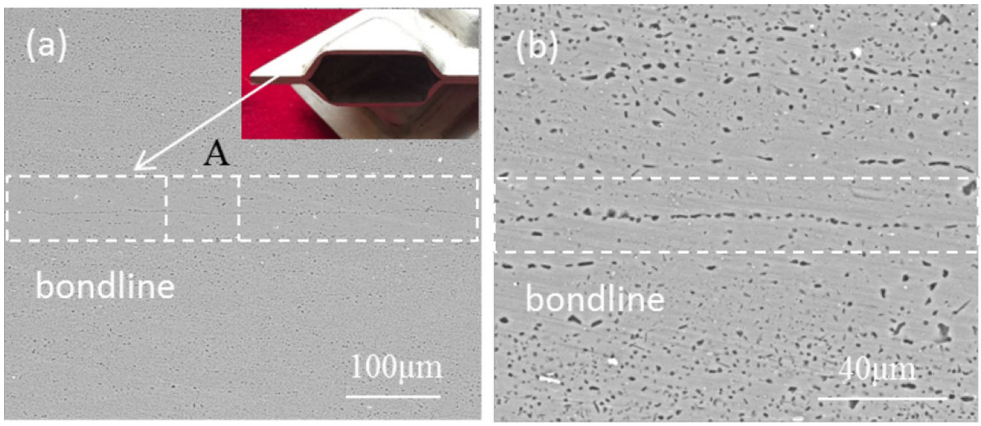

Fig. 16 (a) SEM images of diffusion bonding joints, and (b) high magnification observations to the squared area A in Fig. 15(a)

3.4.2 Microstructure of the Hollow Double-Layer Structure. The SEM image of diffusion bonding joints is shown in Fig. 16. The results showed that a sound bond was obtained in which no discontinuity existed.

4. Conclusions

The SPF/DB process of hollow double-layer structure for 5A90 Al-Li alloy was investigated, and the following conclusion can be drawn:

1. At the temperature of 400 °C and strain rate of 0.001 s^{-1}, the 5A90 Al-Li alloy exhibited superplasticity with elongation of 243.97%.
2. The bonding ratio of the 5A90 Al-Li alloy joints was improved remarkably with the increase in the diffusion bonding temperature and the holding time. Higher bonding temperature and longer holding time can increase the bonding area.
3. Appropriate surface asperities parameter was vital for the localized crushing of aluminum oxide layer on diffusing interface. The diffusion bonding interface did not provide sufficient contact region with surface roughness Ra23, and for the surface roughness Ra13, the micro-plastic deformation on the bond interface was insufficient for the ruptures of the oxide layer. Surface roughness Ra18 was appropriate for the required micro-plastic deformation considering the bonding condition.
4. The hollow double-layer structure of 5A90 Al-Li alloy was manufactured, showing that no voids and unbonding were found at the bond interface, and the thickness of the diffusion bonding area was uniform.

Acknowledgments

This work has been supported by the National Natural Science Foundation of China (No. 51305100), the National Science and Technology Major Project of China, the Project No. is 2014ZX04001-141.

References

1. R.J. Rioja and J. Liu, The Evolution of Al-Li Base Products for Aerospace and Space Applications, *Metall. Mater. Trans. A*, 2012, **43**, p 3325–3337
2. R.K. Gupta, N. Nayan, G. Nagasireesha, and S.C. Sharma, Development and Characterization of Al-Li Alloys, *Mater. Sci. Eng. A*, 2006, **420**, p 228–234
3. E.A. Starke, Jr., T.H. Sanders, Jr., and I.G. PalmerNew, Approaches to Alloy Development in the AI-Li System, *JOM*, 1981, **33**, p 24–33
4. D.V. Dunford and P.G. Partridge, Diffusion Bonding of Al-Li Alloys, *Mater. Sci. Technol*, 1992, **8**, p 385–398
5. A. Urena, J. DeSalazar, J. Quinones, and J. Martin, Tem Characterization of Diffusion Bonding of Superplastic 8090 Al-Li Alloy, *Scr. Mater*, 1996, **34**, p 617–623
6. P.G. Partridge, Oxidation of Aluminium–Lithium Alloys in the Solid and Liquid States, *Int. Mater, Rev*, 1990, **35**, p 37–58
7. P. Zhang, L. Ye, X. Zhang, G. Gu, H. Jiang, and Y. Wu, Grain Structure and Microtexture Evolution During Superplastic Deformation of 5A90 Al-Li Alloy, *Trans. Nonferrous Metal. Soc.*, 2014, **24**, p 2088–2093
8. Y. Huang, N. Ridley, F.J. Humphreys, and J.Z. Cui, Diffusion Bonding of Superplastic 7075 Aluminium Alloy, *Mater. Sci. Eng. A*, 1999, **266**, p 295–302
9. H. Wu, Influence of Process Variables on Press Bonding of Superplastic 8090 Al-Li Alloy, *Mater. Sci. Eng. A*, 1999, **264**, p 194–200
10. C.J. Gilmore, D.V. Dunford, and P.G. Partridge, Microstructure of Diffusion-Bonded Joints in AI-Li 8090 Alloy, *J. Mater. Sci.*, 1991, **26**, p 3119–3124
11. J. Wadsworth, I.G. Palmer, and D.D. Crooks, Superplasticity in Al-Li Based Alloys, *Scr. Metall.*, 1983, **17**, p 347–352
12. M.C. Pandey, J. Wadsworth, and A.K. Mukherjee, Cavitation Study on Ingot and Powder Metallurgically Processed Superplastic AI-Li Alloys, *Mater. Sci. Eng*, 1986, **78**, p 115–125
13. H. Somekawa, H. Watanabe, T. Mukai, and K. Higashi, Low Temperature Diffusion Bonding in a Superplastic AZ31 Magnesium Alloy, *Scr. Mater.*, 2003, **48**, p 1249–1254
14. A. Hill and E.R. Wallach, Modelling Solid-State Diffusion Bonding, *Acta Metall.*, 1989, **37**, p 2425–2437
15. T. Nieh, J. Wadsworth, and O.D. Sherby, *Superplasticity in Metals and Ceramics*, Cambridge University Press, Cambridge, 2005
16. N. Orhan, M. Aksoy, and M. Eroglu, A New Model for Diffusion Bonding and Its Application to Duplex Alloys, *Mater. Sci. Eng. A*, 1999, **271**, p 458–468